Biochimica et Biophysica Acta 1827 (2013) 1245–1255

Contents lists available at ScienceDirect

Biochimica et Biophysica Acta

journal homepage: www.elsevier.com/locate/bbabio

Mitochondrial glutamate carriers from *Drosophila melanogaster*: Biochemical, evolutionary and modeling studies

Paola Lunetti [a], Anna Rita Cappello [b], René Massimiliano Marsano [c], Ciro Leonardo Pierri [d,e], Chiara Carrisi [a], Emanuela Martello [b], Corrado Caggese [c,*], Vincenza Dolce [b,**,1], Loredana Capobianco [a,***,1]

[a] Department of Biological and Environmental Sciences and Technologies, University of Salento, 73100 Lecce, Italy
[b] Department of Pharmacy, Health and Nutritional Sciences, University of Calabria, 87036 Arcavacata di Rende, Cosenza, Italy
[c] Department of Biology, University of Bari, 70125 Bari, Italy
[d] Department of Biosciences, Biotechnology and Biopharmaceuticals, University of Bari, 70125 Bari, Italy
[e] Center of Excellence in Comparative Genomics, University of Bari, 70125 Bari, Italy

ARTICLE INFO

Article history:
Received 11 February 2013
Received in revised form 26 June 2013
Accepted 2 July 2013
Available online 11 July 2013

Keywords:
Drosophila melanogaster
CG18347 and *CG12201*
Proteomics
Glutamate carrier
Phylogenesis

ABSTRACT

The mitochondrial carriers are members of a family of transport proteins that mediate solute transport across the inner mitochondrial membrane. Two isoforms of the glutamate carriers, GC1 and GC2 (encoded by the *SLC25A22* and *SLC25A18* genes, respectively), have been identified in humans. Two independent mutations in *SLC25A22* are associated with severe epileptic encephalopathy. In the present study we show that two genes (*CG18347* and *CG12201*) phylogenetically related to the human GC encoding genes are present in the *D. melanogaster* genome. We have functionally characterized the proteins encoded by *CG18347* and *CG12201*, designated as *Dm*GC1p and *Dm*GC2p respectively, by overexpression in *Escherichia coli* and reconstitution into liposomes. Their transport properties demonstrate that *Dm*GC1p and *Dm*GC2p both catalyze the transport of glutamate across the inner mitochondrial membrane. Computational approaches have been used in order to highlight residues of *DmGC1p* and *DmGC2p* involved in substrate binding. Furthermore, gene expression analysis during development and in various adult tissues reveals that *CG18347* is ubiquitously expressed in all examined *D. melanogaster* tissues, while the expression of *CG12201* is strongly testis-biased. Finally, we identified mitochondrial glutamate carrier orthologs in 49 eukaryotic species in order to attempt the reconstruction of the evolutionary history of the glutamate carrier function. Comparison of the exon/intron structure and other key features of the analyzed orthologs suggests that eukaryotic glutamate carrier genes descend from an intron-rich ancestral gene already present in the common ancestor of lineages that diverged as early as bilateria and radiata.

1. Introduction

Many metabolic pathways require a flux of metabolites into or from the mitochondrial matrix. The selective transport of metabolites with a molecular mass > 5 kDa across the inner mitochondrial membrane is mediated by mitochondrial carriers (MCs), a family of proteins (InterPro entry: IPR018108, PANDIT: PF00153) encoded by nuclear genes [1]. All the members of this family have a tripartite structure consisting of three tandemly repeated sequences of about 100 amino acids in length. Each repeat contains two hydrophobic stretches that span the membrane as α-helices and the characteristic signature motif P-X-[D/E]-X-X-[K/R]-X-[R/K]- 20/30 residues -[D/E]-G-X-X-X-X-[W/Y/F]-[K/R]-G. A mitochondrial carrier of particular interest for human pancreas, liver and brain function is the glutamate carrier (GC). In *Homo sapiens*, two genes (*SLC25A22* and *SLC25A18*) encoding GC1 and GC2, respectively, have been identified [2]. Both are ubiquitous, but *SLC25A22* is expressed at higher amounts in all tissues and is particularly abundant in liver and pancreas. The two isoforms of the glutamate carrier have distinct kinetic parameters [2], although they transport the same substrate. The differences in expression levels and kinetic parameters suggest that GC2 matches the basic requirement of all tissues, especially with respect to amino acid degradation, and that GC1 becomes operative to accommodate higher demands associated with specific metabolic functions [3]. Because glutamate is co-transported with an H^+ by the GC, and therefore its

Abbreviations: GC, glutamate carrier; *Dm*GC1, *Drosophila melanogaster* glutamate carrier isoform 1; *Dm*GC2, *Drosophila melanogaster* glutamate carrier isoform 2; HEPES, (4-(2-hydroxyethyl)-1-piperazineethanesulfonic acid); MES, 2-(*N*-morpholino)ethanesulfonic acid; NRG, nuclear respiratory gene; SDS-PAGE, polyacrylamide gel electrophoresis in the presence of sodium dodecyl sulfate

* Correspondence to: C. Caggese, Department of Biology, University of Bari, Via Orabona 4, 70125 Bari, Italy. Tel.: +39 0 805443393; fax: +39 0 805443386.
** Corresponding author. Tel.: +39 0 984493177; fax: +39 0 984493107.
*** Corresponding author. Tel.: +39 0832298864; fax: +39 0 832298626.
E-mail addresses: corrado.caggese@uniba.it (C. Caggese), vincenza.dolce@unical.it (V. Dolce), loredana.capobianco@unisalento.it (L. Capobianco).
[1] Joint senior authors.

0005-2728/$ – see front matter © 2013 Elsevier B.V. All rights reserved.
http://dx.doi.org/10.1016/j.bbabio.2013.07.002

distribution across the mitochondrial membrane is dependent on ΔpH, entry of glutamate is favored in energized mitochondria. However, when glutamate is generated intramitochondrially (e.g., by proline oxidation), the GC may operate in the reverse direction to limit intramitochondrial accumulation of glutamate [3].

The GCs play important roles in amino acid degradation, nitrogen metabolism, urea synthesis and insulin secretion [2,4,5]. It is believed that the biochemical/physiological role of the glutamate carrier is to provide glutamate for the production of NH_3 via glutamate dehydrogenase, which is exclusively located in the mitochondria as determined in rat liver mitochondria experiments [6,7]. Notably, glutamate entering on the glutamate/aspartate antiporter is necessarily transaminated with intramitochondrial oxaloacetate to form aspartate and is hence not available to the glutamate dehydrogenase [6]. Furthermore, Casimir et al. (see ref. [5]) demonstrated that insulin-secreting cells depend on GC1 (SLC25A22) for maximal glucose response, thereby assigning a physiological function to the newly identified mitochondrial glutamate carrier. Recently, genetic and sequencing analyses have led to the identification of two independent missense mutations in the *SLC25A22* gene that change two highly conserved amino acid residues in GC1 and are responsible for an autosomal recessive form of early infantile epileptic encephalopathy [8].

It was also proposed that GC1-dependent epilepsy was due to a defect of mitochondrial glutamate transport in astrocytes, which would consequently lead to an increase in intrasynaptic glutamate concentration, thus GCs in brain cell mitochondria appear to play a crucial role in the control of intrasynaptic glutamate concentration [3].

Despite its metabolic importance, the mitochondrial glutamate carrier has not yet been identified or characterized in model organisms. In the present study, we report on *Dm*GC1p and *Dm*GC2p, two GC isoforms in *Drosophila melanogaster* encoded by *CG18347* and *CG12201*. In particular, we describe (i) the heterologous expression and purification of *Dm*GC1p and *Dm*GC2p; (ii) the functional characterization of the overexpressed proteins after their incorporation into liposomes; (iii) the expression profile of the two *D. melanogaster* glutamate carriers in different developmental stages and various tissues; (iv) results of an *in silico* analysis aiming to clarify the evolutionary history of the glutamate carrier function in eukaryotes; and (v) computational studies conducted to investigate the glutamate-binding sites of *Dm*GC1 and *Dm*GC2.

2. Material and methods

2.1. Blast search of homologs of the human GC-encoding genes in D. melanogaster and other species

The FlyBase web server (http://flybase.org/) was screened with the sequences of the human isoforms of the mitochondrial GCs [2] for homologous *D. melanogaster* sequences, using the blastp algorithm (http://flybase.org/blast/). Subsequently, BLAST searches of contigs, scaffold and ESTs were performed using *D. melanogaster* CDSs and/or peptides as queries to identify putative glutamate carrier genes in the genome of other Drosophilidae and several other non-Drosophilidae species. These searches were performed using the following databases:

1. the database at the FlyBase web server for *Drosophila simulans*, *Drosophila sechellia*, *Drosophila yakuba*, *Drosophila erecta*, *Drosophila ananassae*, *Drosophila pseudoobscura*, *Drosophila persimilis*, *Drosophila willistoni*, *Drosophila mojavensis*, *Drosophila virilis*, *Drosophila grimshawi* (Drosophila 12 Genomes Consortium, 2007); *Drosophila ficusphila*, *Drosophila eugracilis*, *Drosophila biarmipes*, *Drosophila takahashii*, *Drosophila elegans*, *Drosophila rhopaloa*, *Drosophila kikkawai*, *Drosophila bipectinata*, *Anopheles darlingi*, *Mayetiola destructor*, *Bombyx mori*, *Danaus plexippus*, *Tribolium castaneum*;
2. the database at the VectorBase web site (http://www.vectorbase.org/) for *Glossina morsitans*, *Anopheles gambiae*, *Aedes aegypti*, *Culex quinquefasciatus*, *Ixodes scapularis* and *Rhodnius prolixus*;
3. the database at the Hymenoptera Genome Database (HGD) web site (http://hymenopteragenome.org/) for *Apis mellifera*, *Apis florea*, *Bombus impatiens*, *Bombus terrestris*, *Megachile rotundata*, *Acromyrmex echinatior*, *Atta cephalotes*, *Camponotus floridanus*, *Harpegnathos saltator*, *Linepithema humile*, *Pogonomyrmex barbatus*, *Solenopsis invicta*, *Nasonia vitripennis*, *Nasonia giraulti* and *Nasonia longicornis*,
4. the database at the National Center for Biotechnology (NCBI) web site (http://blast.ncbi.nlm.nih.gov/Blast.cgi) for *Acyrthosiphon pisum*, *Nematostella vectensis* and *Hydra magnipapillata*.

In some of the species investigated the search did not identify any sequences with significant homology to our query sequence, presumably because of gaps or errors in the sequence assemblies. In these cases, we performed BLASTN searches against the shotgun traces available at the NCBI Trace Archive and manually assembled single trace sequences. To identify the most likely glutamate carrier counterparts in different species the "reciprocal best hit" approach was used. In this approach, a common evolutionary origin is assumed if two gene sequences in the compared genomes represent each other the best BLAST hit [9]. To confirm a common ancestor conservation of specific combinations of domains were also considered. Finally, each genomic sequence identified by the criteria reported above was searched manually for exon/intron boundaries to predict the gene transcript *in silico*. The list of the identified GC genes with their positions in different genomes is shown in Supplemental Table S1. Multi-alignments of amino acids and of coding and non-coding sequences were obtained using the MultAlin 5.4.1 software available from the MultAlin server (http://multalin.toulouse.inra.fr/multalin/). To identify nuclear respiratory gene (NRG) elements [10] and other conserved elements in the non-coding sequences of Drosophilidae GC genes, we aligned the orthologous genes, manually identified exon/intron boundaries, and searched for DNA stretches that were highly conserved in all the species studied. To identify NRG motifs in non-Drosophilidae species the Regulatory Sequence Analysis Tools from the RSAT server (http://rsat.ulb.ac.be/) was used.

2.2. Construction of the expression plasmids coding for DmGC1p and DmGC2p

Total RNA was extracted from Oregon-R white pupae flies using the RNeasy Mini Kit (Qiagen, Milan, Italy) and reverse transcribed as described previously [11,12]. The coding regions for *Dm*GC1 and *Dm*GC2 were amplified from cDNA by PCR with 5′-TAGCATATGT CGAGCAGTGCAACCAT-3′ (sense primer) and 5′-CGAAAGCTTCTTTTT CTGATAGCCCAGCAG-3′ (antisense primer) and with 5′-TAGCATAT GTTGGAACAAGTTGAGCAAA-3′ (sense primer) and 5′-CGAAAGCTTC ACAGATTTCGTTCGCTCGA-3′ (antisense primer) of the *D. melanogaster* transcripts *CG18347* and CG12201, respectively. The forward and reverse primers carried *Nde*I and *Hind*III restriction sites, respectively, as linkers. The reaction products were recovered from the agarose gel, cloned into the modified expression vector pET-21b/V5-His [13] and transformed into *E. coli* TG1 cells. Transformants, selected on LB plates containing ampicillin (100 μg/ml), were screened by direct colony PCR and by restriction digestion of purified plasmids. The sequences of the inserts were verified. *Dm*GC proteins were overexpressed as inclusion bodies in *E. coli* Rosetta gami B(DE3) [14,15]. The absence of the stop codon in the reverse primer sequences led to the expression of *Dm*GC proteins fused to carboxy-terminal V5- and His6-epitope tags. Inclusion bodies were isolated by sucrose density gradient and purified by centrifugation and Ni^+-NTA agarose affinity chromatography, as described previously [16–18].

2.3. Reconstitution into liposomes and transport assays

The recombinant proteins in sarkosyl were reconstituted into liposomes in the presence or absence of substrates [19,20]. The reconstitution mixture contained purified proteins (100 μl with 0.5–1 μg of protein), 10% Triton X-114 (90 μl) [21], 10% phospholipids as sonicated liposomes (90 μl), 10 mM glutamate (except where otherwise indicated), 50 mM MES/50 mM HEPES at pH 6.5 (except where otherwise indicated) and water to a final volume of 700 μl. These components were mixed thoroughly, and the mixture was recycled 13 times through the same Amberlite column (Bio-Rad) [22,23]. External substrate was removed from proteoliposomes on Sephadex G-75 columns, pre-equilibrated with 100 mM sucrose and 10 mM MES/10 mM HEPES at pH 6.5 (except where otherwise indicated). Transport at 25 °C was started by adding, at the indicated concentrations, L-[^{14}C]glutamate (Scopus Research BV, Wageningen, Netherlands) to substrate-loaded proteoliposomes (exchange) or to empty proteoliposomes (uniport). In both cases, transport was terminated by the addition of 30 mM PLP. In control samples, the inhibitors were added at time 0 according to the inhibitor stop method [24,25]. Finally, the external substrate was removed and the radioactivity in the liposomes was measured. The experimental values were corrected by subtracting control values. The initial transport rate was calculated from the radioactivity taken up by proteoliposomes after 1 min (in the initial linear range of substrate uptake).

2.4. Expression analysis by real-time PCR

Oregon-R flies were raised on standard culture medium at 24 °C. Total RNA for gene expression analysis was obtained from 0.5- to 1-g samples of Oregon-R individuals at various developmental stages (embryos, larvae, pupae and adult flies). Except for ovaries and testes, male and female tissues contributed equally to each dissection. As the malpighian tubules are bilaterally asymmetric, particular care was taken to include equal numbers of anterior and posterior tubules in each sample. Total RNA from all developmental stages and tissues was isolated using Trizol. RNA was quantified using a Nanodrop spectrophotometer (Thermo Scientific) and diluted to 1 mg/ml for real-time PCR analysis. RNA (1 μg) was reverse transcribed using the Quantitect reverse transcription kit (QIAGEN) according to the protocol supplied by the manufacturer. Primers used for real time amplification were:

*CG18347*U 5′-TCTTCCCACTGGACTTGGTC-3′
*CG18347*L 5′-GTACGTCTTGCGGAAGCAAT-3′
CG12201U 5′-CAAGTTGAGCAAAAGAACCAAG-3′
CG12201L 5′-ACGCATGCCACTCCAATAAT-3′
RpL32U 5′-CGGATCGATATGCTAAGCTGT-3′
RpL32L 5′-CGACGCACTCTGTTGTCG-3′.

Quantitative real-time PCR was achieved with 1 μl cDNA and analyzed in a 7300 Real Time PCR System (Applied Biosystems). Reactions were performed in 10 μl total volume in 94-well plates and consisted of 5 μl of Power SYBR Green PCR Master Mix (Applied Biosystems), 3 pmol forward and reverse primers, and 10 ng total RNA template. All reactions were performed at least in triplicate. Specificity and identity of the amplification products were confirmed by analysis of the dissociation curves. ΔCt values were obtained using the RpL32 housekeeping gene as the internal control. ΔCt values were obtained using the expression data from heads or from embryos as calibrators [26].

2.5. Comparative modeling and substrate binding site investigations

Computational approaches for protein function investigations [27] have been employed to investigate *D. melanogaster* GC protein function. A multiple sequence alignment (MSA) of *Dm*GC1p and *Dm*GC2p and human GC MCs was obtained by using ClustalW and the sequence of the crystallized bovine ADP/ATP carrier (AAC) [28], to insert gaps in the MSA [27,29]. The characterizing triplet set of *Dm*GCs was obtained by aligning the three repeats of the MCs analyzed [30]. Comparative structural models of *Dm*GC1p and *Dm*GC2p were built by using the structure of AAC (PDB ID: 1okc) in complex with its powerful inhibitor carboxyatractyloside as template [28] and Modeller (http://salilab.org/modeller/) as performed for other MCs [31–33]. The structural properties of *Dm*GC1p and *Dm*GC2p comparative models with the best energy function were evaluated using the biochemical/computational tools of the WHAT IF Web server (http://swift.cmbi.ru.nl/whatif/). Q-site Finder (http://bmbpcu36.leeds.ac.uk/qsitefinder/help.html) was used to predict the potential binding sites of the *Dm*GC1p and *Dm*GC2p best models.

2.6. Other methods

Proteins were analyzed by SDS-PAGE and stained with Coomassie blue dye. The amount of recombinant pure *Dm*GC proteins was estimated by laser densitometry of stained samples using carbonic anhydrase as a protein standard [34,35]. The identity of purified *Dm*GC1p and *Dm*GC2p was assessed by MALDI-TOF MS of trypsin digests of the corresponding bands excised from a Coomassie blue-stained gel [36]. The amount of proteins incorporated into liposomes was measured as described previously [37] and was proved to be approximately 20% of the protein added to the reconstitution mixture.

3. Results

3.1. Identification of the D. melanogaster glutamate carrier genes

Using BLAST to search the *D. melanogaster* genome two proteins, *Dm*GC1p and *Dm*GC2p, encoded by *CG18347* and *CG12201*, respectively, and sharing significant homology with the human GC proteins [2] were identified. The *CG18347* and *CG12201* genes are located in a tandem configuration at salivary band 87A7 of chromosomal arm 3R (Fig. 1). The transcript of *CG18347* contains an ORF of 966 bp encoding a protein of 321 amino acid residues with a molecular mass of 34.5 kDa indicated as *Dm*GC1p. The transcript of *CG12201* contains an ORF of 960 bp encoding a protein of 319 amino acid residues with a molecular mass of 34.9 kDa indicated as *Dm*GC2p. The amino acid identity is 63% between Drosophila *Dm*GC1p and *Dm*GC2p, 53% between Drosophila *Dm*GC1p and human GC1, 49% between Drosophila *Dm*GC1p and human GC2, 47% between Drosophila *Dm*GC2p and human GC1, and 43% between Drosophila *Dm*GC2p and human GC2. Human GC1 and GC2 share 63% identity. Prediction programs identified the tripartite structure and the sequence motif typical of the MC family in both *Dm*GC1p and *Dm*GC2p. Furthermore, the alignment of the amino acid sequences of GC1, GC2, *Dm*GC1p, *Dm*GC2p and bovine AAC [28] highlights the conservation of these proteins (Fig. 2).

3.2. Bacterial expression of DmGC proteins

*Dm*GC1p and *Dm*GC2p were overexpressed at high levels in *E. coli* Rosetta gami B(DE3) as inclusion bodies and purified by Ni^{+}-NTA-agarose affinity chromatography (supplementary material, Fig. S1, lanes 3 and 5). The identity of the purified proteins (supplementary material, Fig. S1, lanes 4 and 6) was confirmed by mass spectrometry analysis of trypsin digests. The apparent molecular masses of the purified proteins were about 34 kDa (calculated values with initiator methionine were 37.3 and 37.8 kDa for *Dm*GC1p and *Dm*GC2p, respectively). The proteins were not detected in bacteria harvested immediately before the induction of expression (supplementary material, Fig. S1, lanes 1 and 2), or in cells harvested after induction but lacking the coding sequence for *Dm*GC1p or *Dm*GC2p in the expression

Fig. 1. Chromosomal organization of the *CG18347* and *CG12201* genes in *D. melanogaster*. (A) The position of the two genes, and their annotated transcripts, on chromosome 3R is shown. (B) Multiple alignment of the *CG18347* gene region encompassing the NRG element in 20 Drosophila species.

vector (data not shown). Approximately 100 mg of each purified protein per liter of culture was obtained.

3.3. Functional characterization of recombinant DmGC1p and DmGC2p

*Dm*GC1p and *Dm*GC2p were reconstituted into liposomes and their transport properties tested in homo-exchange experiments (i.e., with the same substrate inside and outside). Using external and internal substrate concentrations of 1 and 10 mM, respectively, both proteins catalyzed an active [^{14}C]glutamate/glutamate exchange but not significant homo-exchanges for aspartate, glutamine, asparagine, phosphate, ADP, ATP, malonate, malate, oxoglutarate, ketoisocaproate, citrate, carnitine, ornithine, lysine, arginine, glutathione, choline, proline, and threonine (data not shown). No [^{14}C]glutamate/glutamate exchange was observed with *Dm*GC1p and *Dm*GC2p that had been boiled before incorporation into liposomes or after reconstitution of sarcosyl-solubilized material from bacterial cells either lacking the expression vector for *Dm*GC1p and *Dm*GC2p or harvested immediately before the induction of expression.

In Fig. 3 the kinetics of uptake into proteoliposomes reconstituted with *Dm*GC1p of 0.5 mM [^{14}C]glutamate measured in the presence (exchange) or absence (unidirectional transport) of 10 mM internal glutamate are shown. Both the exchange and uniport reactions followed first-order kinetics with isotopic equilibrium being approached exponentially. Maximum uptake was approached after 45 min. The corresponding values at infinite time were 25.8 and 1.41 μmol/mg of protein. The ratio of maximal substrate uptake by exchange and by uniport was 18.3, in agreement with the value of 20 expected from the intraliposomal concentrations at equilibrium (10 and 0.5 mM for exchange and uniport, respectively). The initial rates of glutamate exchange and uniport deduced from the respective time courses were 3.87 and 0.49 μmol/min/mg of protein, respectively. The addition of

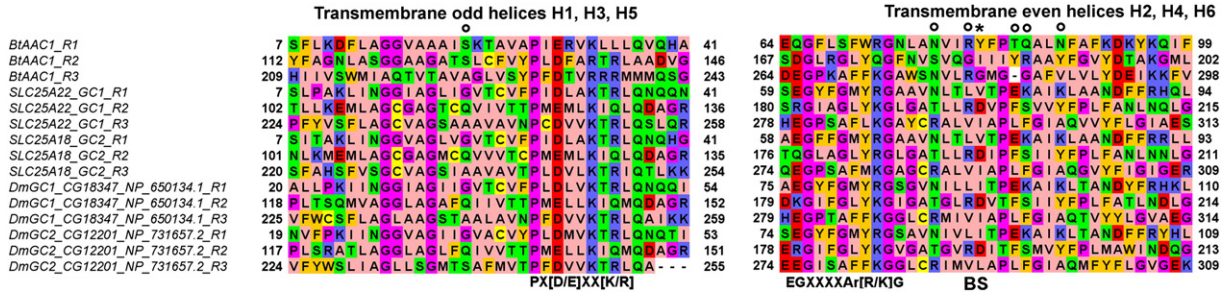

Fig. 2. Inter repeat sequece alignment of Drosophila and human GC carriers. Multiple sequence alignment of the three repeats (R1–3) of *Drosophila melanogaster*, human glutamate carriers (*Dm*GC1_R1-3, *Dm*GC2_R1-3, SLC25A22_GC1_R1-3, SLC25A18_GC2_R1-3) and of the three repeats of the bovine ADP/ATP carrier (BtAAC1_R1-3). For each carrier and each repeat (R1, R2, R3) only the odd transmembrane helices (H1, H3, H5) and the even transmembrane helices (H2, H4, H6) preceded by 10 amino acids are shown. Amino acids are colored according to the default Jalview Zappo style (http://www.jalview.org/). The labels PX[D/E]XX[K/R], EGXXXXAr[R/K]G and BS indicate the position of the first part of the sequence motif, the second part of the sequence motif and the contact points of the proposed substrate binding site [48]. Circles "°" indicate the positions of the characterizing amino acid triplets of the MC GC subfamily, e.g. the first "°" indicates vertical triplet 22 (SSA in BtAAC1 and GQ[A/S] in *Dm*GC1 and *Dm*GC2, respectively) [63]; asterisk "*" indicates the position of vertical triplet 81 (e.g., YIG in BtAAC1 and ID[I/L] in *Dm*GC1 and *Dm*GC2, respectively).

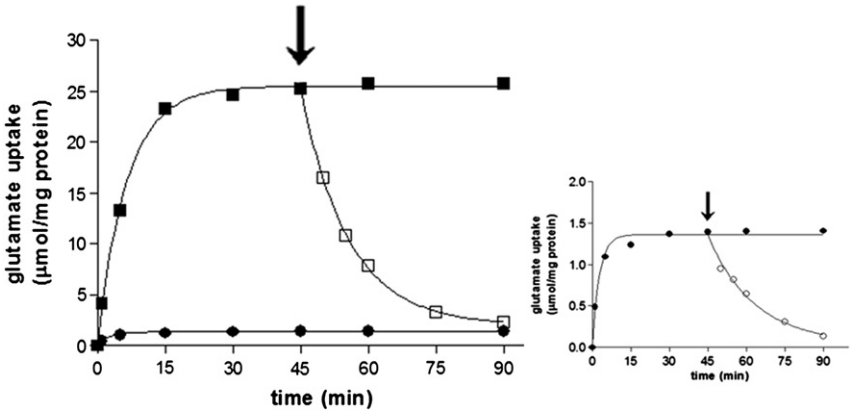

Fig. 3. Kinetics of [^{14}C]glutamate uniport and [^{14}C]glutamate/glutamate exchange by *Dm*GC1p. Proteoliposomes were reconstituted with *Dm*GC1p. 0.5 mM [^{14}C]glutamate was added to proteoliposomes containing 10 mM glutamate (exchange, ■) or 10 mM NaCl and no substrate (uniport, ●). The arrow indicates the addition of 10 mM nonradioactive glutamate (□ and ○). Similar results were obtained in four independent experiments.

10 mM unlabeled glutamate to proteoliposomes after incubation with 0.5 mM [^{14}C]glutamate for 45 min, when radioactive uptake had almost approached equilibrium, caused an extensive efflux of radiolabeled glutamate from both glutamate-loaded and unloaded proteoliposomes (Fig. 3). This efflux shows that [^{14}C]glutamate taken up by exchange or unidirectional transport is released in exchange with externally added substrate. Similar data were obtained using *Dm*GC2p instead of *Dm*GC1p (data not shown). Therefore, *Dm*GC1p and *Dm*GC2p catalyze both unidirectional transport of glutamate and glutamate/glutamate exchange, as reported for recombinant human GCs [2] and glutamate transport in isolated mitochondria [4].

The substrate specificity of recombinant *Dm*GC1p and *Dm*GC2p was examined in detail by measuring the uptake of [^{14}C]glutamate into proteoliposomes preloaded with various potential substrates (Table 1). With both proteins, external L-glutamate was exchanged significantly only in the presence of internal L-glutamate. With *Dm*GC1p, a low exchange was found with α-methyl-DL-glutamate, L-aspartate and L-α-aminoadipate, while the activity observed in the presence of internal L-α-aminopimelate, L-cysteinesulfinate, L-glutamine, L-asparagine, glutarate and adipate was approximately the same as that observed in the absence of internal substrate (Table 1). Isoform *Dm*GC2p was more specific, as virtually no exchange activity was detected in the presence of internal α-methyl-DL-glutamate, L-aspartate, L-α-aminoadipate, L-α-aminopimelate, L-cysteinesulfinate, L-glutamine, L-asparagine, glutarate and adipate (Table 1). Reconstituted *Dm*GC1p and *Dm*GC2p, therefore, exhibit a very narrow substrate specificity, which is virtually confined to L-glutamate.

Table 1
Dependence on internal substrate of the transport properties of proteoliposomes reconstituted with recombinant *Dm*GC1p and *Dm*GC2p.
Proteoliposomes were preloaded internally with various substrates (concentration 10 mM). Transport was started by adding 0.5 or 1 mM [^{14}C]glutamate to proteoliposomes reconstituted with *Dm*GC1p or *Dm*GC2p, respectively, and terminated after 3 min. Similar results were obtained in at least four independent experiments.

Internal substrate	[^{14}C]Glutamate transport	
	*Dm*GC1p	*Dm*GC2p
	µmol/min/mg of protein	
None (Cl^- present)	0.50	0.12
L-glutamate	4.31	1.19
α-methyl-DL-glutamate	1.38	0.12
L-aspartate	0.90	0.15
L-α-aminoadipate	0.86	0.13
L-α-aminopimelate	0.56	0.12
L-cysteinesulfinate	0.43	0.13
L-glutamine	0.49	0.13
L-asparagine	0.50	0.12
Glutarate	0.51	0.13
Adipate	0.49	0.13

The [^{14}C]glutamate/glutamate exchange reactions catalyzed by reconstituted *Dm*GC1p and *Dm*GC2p were almost completely inhibited by *p*-hydroxymercuribenzoate, mersalyl and pyridoxal 5′-phosphate, inhibitors of several MCs [38,39]. Both *Dm*GC1p and *Dm*GC2p were also inhibited markedly by *N*-ethylmaleimide, tannic acid and bromocresol purple (Fig. 4). In contrast, bathophenanthroline, another known inhibitor of several MCs [40,41] affected the reconstituted transport activities poorly. In addition, no significant inhibition was observed with bongkrekate [11] and 1,2,3-benzenetricarboxylate [24,42], which are specific inhibitors of the AAC and citrate carrier, respectively.

3.4. Influence of the pH gradient on the uptake of glutamate by DmGCs

Because glutamate is transported across the mitochondrial membrane together with H^+ [4], the influence of the proton gradient on the *Dm*GC1p-catalyzed uptake of glutamate into liposomes was investigated. The liposomes were reconstituted at various pH values (from 6.5 to 8.0) and with no internal substrate. After removal of the external buffer by passage through Sephadex G-75, [^{14}C]glutamate (buffered at pH 6.5) was added to the proteoliposomes, and the initial rate of uptake was measured. The results in Fig. 5 show that the rate of glutamate uptake mediated by both *Dm*GC1p and *Dm*GC2p increases 3–4 times with the increase of internal pH from 6.5 to 8 (at a fixed external pH of 6.5). In constrast, the rate of the glutamate/glutamate exchange was little affected by changing the internal pH from 6.5 to 8.0 (data not shown). These results are similar to those described in studies with intact mitochondria [4] and with human GCs [2] and are in agreement with the notion that the mitochondrial GC catalyzes a glutamate + H^+ co-transport.

3.5. Kinetic properties

The kinetic constants of the recombinant purified *Dm*GC1p and *Dm*GC2p were determined by measuring the initial transport rate at various external [^{14}C]glutamate concentrations in the presence of a constant saturating internal concentration (10 mM) of glutamate (glutamate/glutamate exchange) (Table 2). At the same internal and external pH of 6.5, the half-saturation constants (K_m) of reconstituted *Dm*GC1p and *Dm*GC2p were 0.40 ± 0.03 and 2.93 ± 0.27 mM, respectively, and the V_{max} values were 7.25 ± 0.69 and 4.29 ± 0.40 µmol/min/mg protein, respectively.

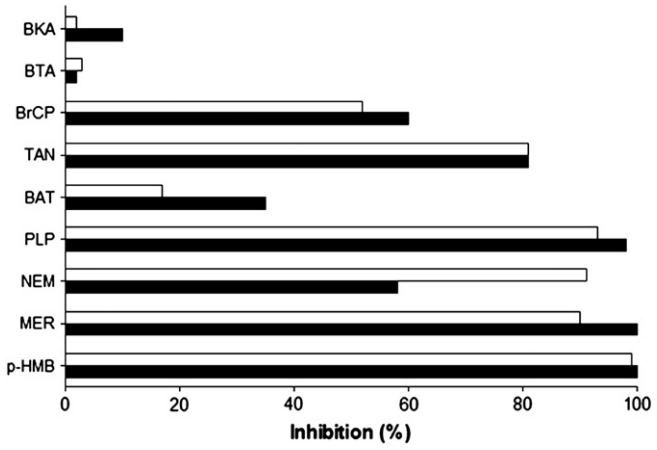

Fig. 4. Effect of inhibitors on the [^{14}C]glutamate/glutamate exchange by *Dm*GC1p and *Dm*GC2p. Proteoliposomes were preloaded internally with 10 mM glutamate. Transport was initiated by adding 0.5 or 1 mM [^{14}C]glutamate to proteoliposomes reconstituted with *Dm*GC1p (filled bars) or *Dm*GC2p (open bars), respectively, and was stopped after 3 min. The inhibitors were added 3 min before the labeled substrate. The final concentrations of the inhibitors were 50 μM (MER, mersalyl; p-HMB, *p*-hydroxymercuribenzoate), 10 mM (PLP, pyridoxal 5′-phosphate; BAT, bathophenanthroline), 1 mM (NEM, *N*-ethylmaleimide), 0.1% (TAN, tannic acid), 0.1 mM (BrCP, bromocresol purple), 2.5 mM (BTA, benzene-1,2,3-tricarboxylate), and 10 μM (BKA, bongkrekic acid). The extent of inhibition (%) from a representative experiment for each carrier is reported. Similar results were obtained in four experiments.

3.6. Expression of D. melanogaster glutamate carrier genes

To determine the expression levels of the *CG18347* and *CG12201* genes, we carried out a quantitative real time RT-PCR analysis on total RNA samples extracted from different Drosophila developmental stages or from tissues dissected from adults (Fig. 6). The results obtained revealed a widely distributed expression of *CG18347* throughout development and in all the adult tissues analyzed. By contrast, the expression of *CG12201* was detectable starting from the late larval/pupal stage and seemed to be male-specific, as confirmed by the high expression level in testis. To obtain additional evidence of the differential expression pattern of the two genes we searched Drosophila EST databases for sequences transcribed from *CG18347* and *CG12201*. With the exception of *D. simulans*, in all other *Drosophila* species the abundance of ESTs originating from *CG12201* was lower than that of ESTs originating from *CG18347* (in total, 31 versus 109 ESTs). Furthermore, the results confirmed that the expression of *CG12201* is strongly testis-biased, as 7 of 9 *CG12201* ESTs were found in testis-derived libraries, while only 1 of the 27 ESTs originating from *CG18347* was found in such libraries, all the others being found in libraries derived from cell cultures or somatic tissues. In support of these results, the search of an EST library from *D. yakuba* testes also showed a testis-biased expression of the ortholog of the *D. melanogaster CG12201* gene (data not shown).

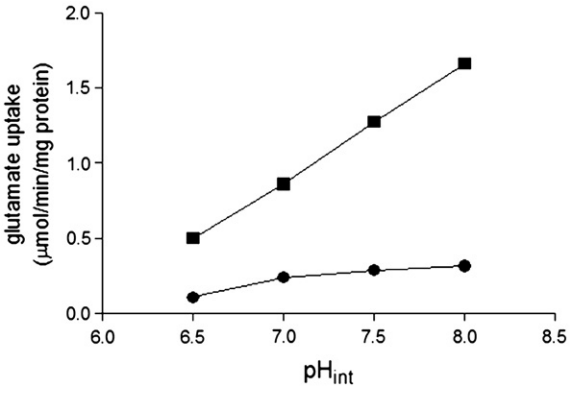

Fig. 5. Dependence on transmembrane pH gradient of [^{14}C]glutamate uptake by *Dm*GC1p and *Dm*GC2p. The reconstitution mixture contained 10 mM NaCl and 50 mM MES/50 mM HEPES at various pH values from 6.5 to 8.0. After reconstitution of *Dm*GC1p (■) or *Dm*GC2p (●) into liposomes, a mixture of 100 mM sucrose and 0.1 mM MES/0.1 mM HEPES at the same pH of the reconstitution mixture was used to equilibrate and to eluate the Sephadex G-75 columns. Transport was started by adding 0.5 mM [^{14}C]glutamate together with 10 mM MES/10 mM HEPES at pH 6.5 to proteoliposomes. The reaction was terminated after 3 min. Similar results were obtained in four independent experiments.

3.7. All eukaryotic mitochondrial glutamate carrier genes have a common evolutionary origin

Sequences with significant homology to the *D. melanogaster CG18347* and *CG12201* genes were found in the genomes of 18 Drosophilidae species, i.e., *D. sechellia*, *D. simulans*, *D. yakuba*, *D. erecta*, *D. ananassae*, *D. pseudoobscura*, *D. persimilis*, *D. willistoni*, *D. virilis*, *D. grimshawi* (Drosophila 12 Genomes Consortium, 2007), *D. ficusphila*, *D. eugracilis*, *D. biarmipes*, *D. takahashii*, *D. elegans*, *D. rhopaloa*, *D. kikkawai*, and *D. bipectinata*. These sequences identified two genes arranged in a conserved tandem configuration, which most likely represent the orthologs of *D. melanogaster CG18347* and *CG12201*. They share with *D. melanogaster* genes not only significant sequence homology, but also a strikingly conserved exon/intron organization, i.e. five coding exons for the *CG18347* orthologs and three coding exons for the *CG12201* orthologs (see Supplemental Table S2). Notably, in the *D. mojavensis* genome *CG12201* was not detected.

As a first step toward understanding the evolutionary history of the GC genes, we compared the Drosophilidae genes with their counterparts in an informative range of other Arthropod species (26 insects and an Ixodida, *I. scapularis*). The species investigated were 6 Diptera, i.e. *G. morsitans* (Tsetse fly), *A. gambiae* (Malaria mosquito), *A. darlingi* (American malaria mosquito), *A. aegypti* (Yellow fever mosquito), *C. quinquefasciatus* (Southern house mosquito), and *M. destructor* (Hessian fly); 2 Lepidoptera, i.e. *B. mori* (silkworm) and *D. plexippus* (monarch butterfly); 1 Coleoptera, *T. castaneum* (red flour beetle); 12 Hymenoptera, i.e. *A. mellifera* (Western honey bee), *A. florea* (Dwarf honey bee), *B. impatiens* (Commoneastern bumblebee), *B. terrestris* (Buff-tailed bumblebee), *M. rotundata* (Alfalfa leafcutter bee), *A. echinatior* (Panamanian leafcutter ant), *A. cephalotes* (Leafcutter ant), *C. floridanus* (Florida carpenter ant), *H. saltator* (Jerdon's jumping ant), *L. humile* (Argentine ant), *P. barbatus* (Red harvester ant), and *S. invicta* (Red fire ant); 3 parasitic wasps: *N. vitripennis*, *N. giraulti* and *N. longicornis*; and 2 Hemiptera: *A. pisum* (pea aphid) and *R. prolixus* (Kissing bug).

In contrast to what is found in Drosophilidae, in the genome of all these species a single GC-encoding gene with structural features related to *D. melanogaster CG18347* was detected. The complete list of the identified GC-encoding genes and their position in the respective genomes is shown in Supplemental Table S3. The few variations in the exon/intron organization of the genes investigated are visualized in Fig. 7 (more details in Supplemental Table S3). Comparison of all the genes investigated and, in particular, those in insects and in Ixodida *I. scapularis* (Deer tick) suggest the existence of a common ancestor before the divergence of the Arthropods; intron loss apparently has occurred in Drosophila, Glossina and Mayetiola, while intron gain suggests a lineage-specific process. In humans, the identical exon/intron organization of the two GC-encoding genes *SLC25A22* and *SLC25A18* (nine coding exons) is consistent with a segmental duplication of an ancestral gene (Fig. 7). How many structural features do the Arthropoda genes share with their human counterparts? Comparison of intron positions, exon phase and exon length indicates that the Arthropod and human genes share a common intron-rich ancestor predating the divergence of these lineages. Because position conservation in multiple Arthropod lineages and in humans can be assumed to identify retained ancestral introns, we infer that the common ancestor

Table 2
Kinetic constants of *Dm*GC1p and *Dm*GC2p.
The values were calculated from double reciprocal plots of the rate of [^{14}C]glutamate uptake versus substrate concentrations into liposomes reconstituted with *Dm*GC1p or *Dm*GC2p. The reconstitution mixture contained 10 mM glutamate (glutamate/glutamate exchange) and 50 mM MES/50 mM HEPES at pH 6.5 or 8.0. After reconstitution of *Dm*GC1p or *Dm*GC2p into liposomes, a mixture of 100 mM sucrose and 0.1 mM MES/0.1 mM HEPES at the same pH of the reconstitution mixture was used to equilibrate and elute the Sephadex G-75 columns. Transport was started by adding [^{14}C]glutamate together with 10 mM MES/10 mM HEPES at pH 6.5 and terminated after 1 min. The externally added substrate concentrations were as follows: 0.01–2 mM for *Dm*GC1p and 0.5–5 mM for *Dm*GC2p. The data represent the means ± S.D. of 6 independent experiments.

	*Dm*GC1p		*Dm*GC2p	
	K_m mM	V_{max} μmol/min/mg	K_m mM	V_{max} μmol/min/mg
Glutamate/glutamate(pH_{in} 6.5)	0.40 ± 0.03	7.25 ± 0.69	2.93 ± 0.27	4.29 ± 0.40
Glutamate/glutamate (pH_{in} 8)	0.36 ± 0.03	6.88 ± 0.60	2.68 ± 0.22	3.98 ± 0.38

gene comprised at least six introns. Finally, the GC-encoding genes in the genomes of two basal metazoans, the Cnidarians *N. vectensis* and *H. magnipapillata*, were also investigated. The single Cnidarian GC-encoding gene comprises six introns in *N. vectensis* and eight in *H. magnipapillata* (Fig. 7 and Supplemental Table S3). Again, conservation of exon/intron organization indicates that a single GC-encoding gene, containing at least eight exons, existed in a common ancestor of Metazoa.

3.8. Conservation of regulatory elements

Interspecific DNA sequence comparison is a useful tool for identifying *cis*-regulatory DNA sequences involved in the regulation of eukaryotic gene expression [43]. We searched for conserved motifs in the noncoding sequences of the Drosophilidae GC genes by phylogenetic footprinting and DNA pattern discovery programs [44]. The NRG element is a palindromic 8-bp motif (TTAYRTAA) known to be shared by all nuclear Insect OXPHOS genes and by many other nuclear genes involved in the biogenesis and function of the mitochondrion [10,45]. In *D. melanogaster*, NRG elements are usually located within an intron downstream of the transcription start site. A TTACGTAA NRG element is found 341 bp downstream of the transcription start site in the first intron of the *D. melanogaster CG18347* gene. This 8-bp motif is extremely conserved and constantly located in its specific position in the first intron in all Drosophilidae *CG18347* orthologs (Fig. 1B). To answer the question whether the NRG element in GC genes is conserved over long evolutionary times, the noncoding regions of the GC genes of the 27 non-Drosophilidae Arthropoda species investigated in this work were also researched. Notwithstanding very long divergence times (the divergence between Drosophilidae and Ixodida is thought to have occurred approximately 500 mya [46], single or multiple NRG elements were detected in the GC genes of the majority of Arthropoda species, and the intragenic localization of such elements is often strictly conserved (not shown). An in-depth

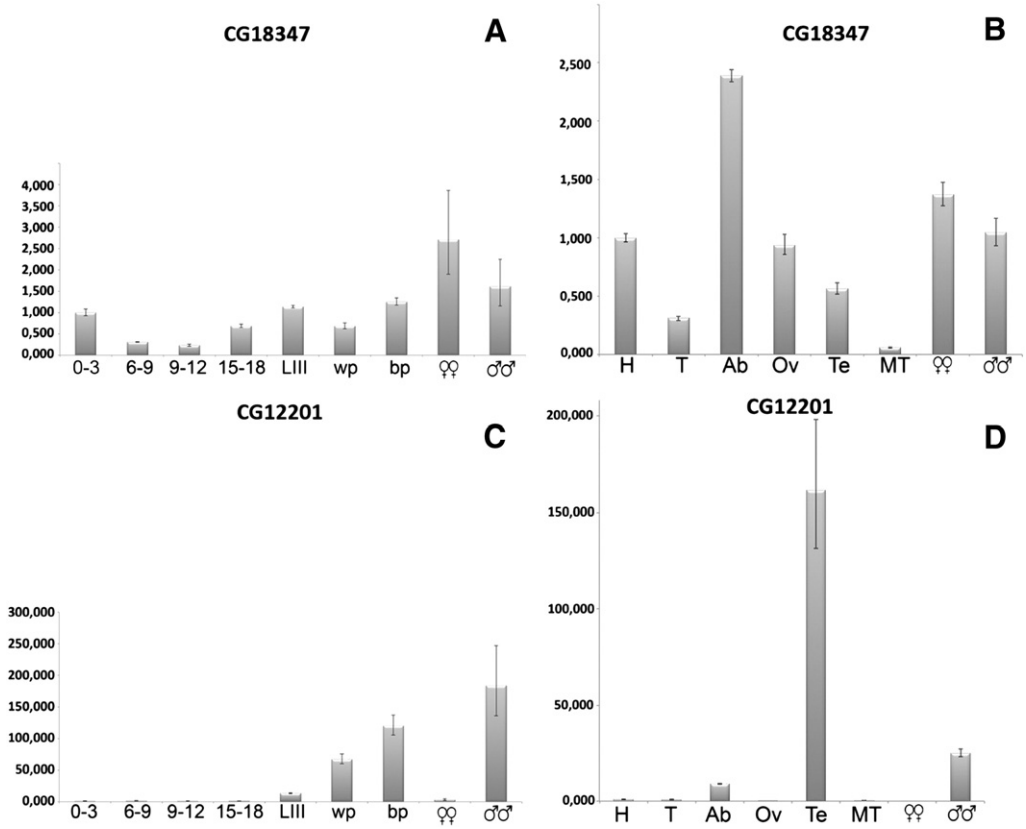

Fig. 6. Transcriptional analysis of *CG18347* and *CG12201* genes. *Dm*GC1 and *Dm*GC2 transcription was analyzed by qRT-PCR through development (panels A and C) and in different tissues (panels B and D). RNA samples were collected from embryos at four stages of embryonic development (0–3, 6–9, 9–12 and 15–18 h after deposition), 3rd instar larvae (LIII), white prepupae (wb), black pupae (bp), and adults (female and male symbols). Tissue samples were collected from heads (H), thoraxes (T), abdomens (Ab), ovaries (Ov), testes (Te), malpighian tubules (MT), and whole adults (female and male symbols).

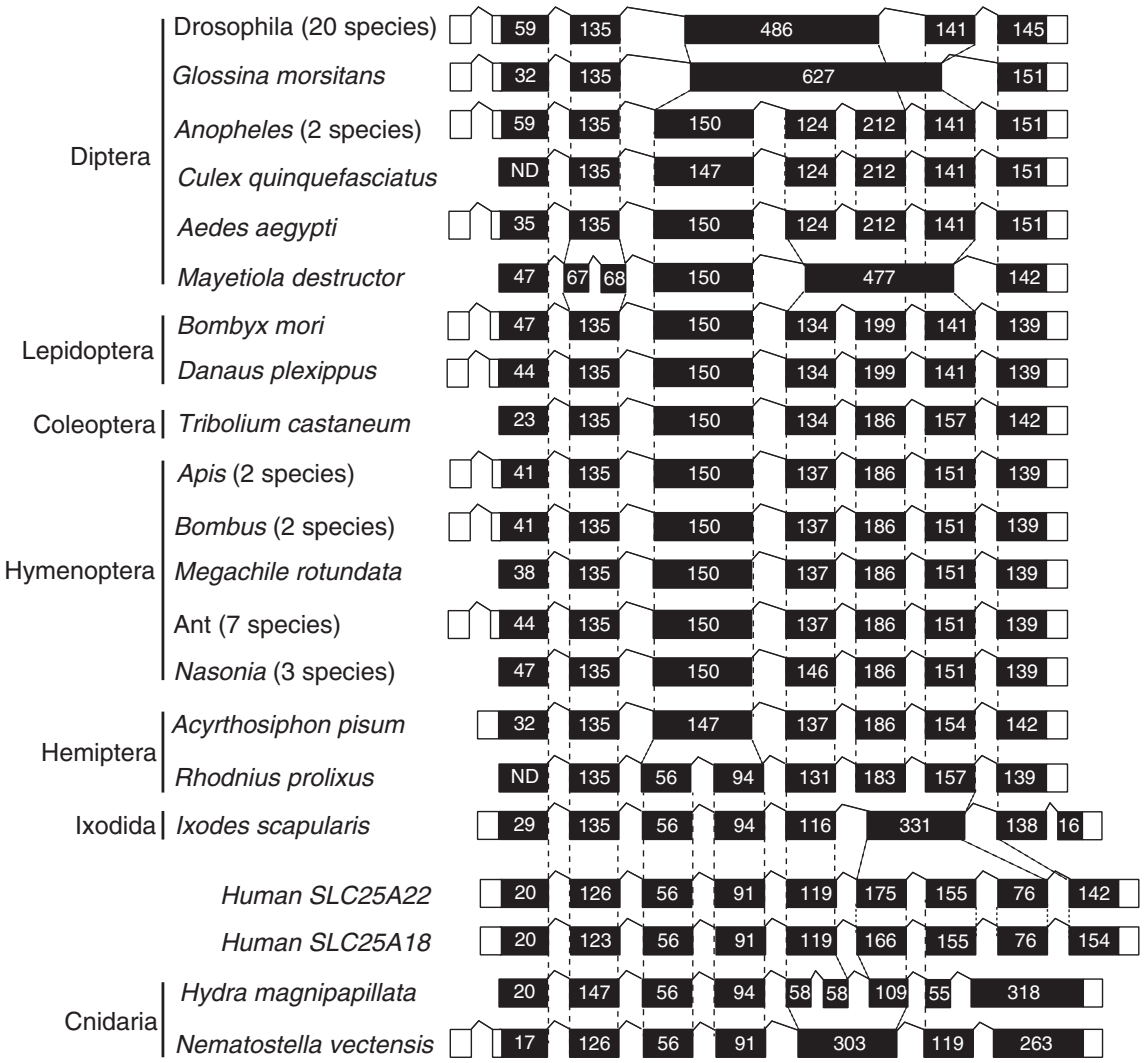

Fig. 7. Eukaryotic GC-encoding genes share an ancient intron-rich ancestor. The pre-mRNAs putatively transcribed from the orthologous GC1-encoding genes of representative eukaryotic species are compared taking into account intron position, exon phase and exon length. Dashed lines indicate conservation of intron position. Translated GC1-encoding regions are indicated in black, UTRs as white boxes. Boxes are not in scale.

analysis of the NRG element position in GC genes whose transcription start site can be inferred from the EST sequences available suggests that single and multiple NRG elements are differently distributed. Single NRG motifs are located 150 to 400 bp downstream of the transcription start site, whereas multiple NRG sites are present in the transcriptional unit with no apparent positional preference, as observed for example in Hymenoptera (Supplemental Table S3).

3.9. Sequence properties and binding sites of DmGC1p and DmGC2p

It has recently been shown that MC subfamilies are characterized not only by their substrate specificity but also by a specific set of amino acid triplets [30]. These triplets consist of the aligned symmetry-related amino acids (Fig. 2) of each carrier when their three repeat sequences are aligned [29,47]. The calculation of the inter-repeat multiple sequence alignment and the construction of a triplet diagram make sequence comparison faster and consequently allow to predict MC function more rapidly, provided that an ortholog of the investigated carrier has been experimentally characterized. To determine the DmGC characterizing triplets, we identified their symmetry-related triplet amino acids and compared them with those proposed for the GC subfamily [30]. Notably, the complete set of characterizing triplets of the mitochondrial GC subfamily [(22 (GQA), 77 (NTR), 80 (LRV), 84 (EFL), 85 (KSF), 88 (KYA)] [30], defined after the identification of the human GCs [2], is conserved in the two *Dm*GCs with only a partial deviation in triplet 22 (Fig. 2). This triplet consists of "GQA" in *Dm*GC1p, as in human GCs, and of "GQS" in *Dm*GC2p. Another interesting difference in triplet composition between human and Drosophila GCs concerns triplet 81, that in *Dm*GC1p is "IDI", like in human GCs [30], whereas in *Dm*GC2p is "IDL". It is worth mentioning that the amino acid in the second position of triplet 81, corresponding to Asp-196 in *Dm*GC1p and to Asp-195 in *Dm*GC2p, is involved in the common substrate binding site of amino acid carriers [29,48] (see below).

By using the Q-site Finder tool we found that the predicted substrate binding sites in *Dm*GC1p and *Dm*GC2p overlap with the 1okc carboxyatractyloside binding region of the crystallized bovine AAC1 and extends between proline–glycine (PG) level 1 and PG level 2, a typical MC area deeply involved in conformational changes occurring during substrate translocation [29]. It should be noticed that this region contains the characteristic charged dipeptide RD (Arg195–Asp196 in *Dm*GC1 and Arg194–Asp195 in *Dm*GC2). This dipeptide, which is shared by many MCs transporting amino acids [48], is localized in transmembrane helix 4 approximately at mid-point of the carrier cavity. Furthermore, these residues have been proposed to participate in the common substrate binding site of MCs [48].

4. Discussion

We used both experimental and theoretical methods for the study of the biochemical and evolutionary features of *Dm*GC proteins as a first step towards the understanding of their role in nitrogen metabolism. Furthermore, in this manuscript a binding pose of the glutamate within glutamate carrier cavities has been proposed for the first time. Glutamate carrier activity has been the object of many studies performed on isolated intact mitochondria [4] and, more recently, after functional reconstitution, on recombinant human proteins overexpressed in *E. coli* [2]. In *D. melanogaster* the GC is involved in specific glutamate uptake for the production of ammonia via glutamate dehydrogenase, which is exclusively located in the mitochondria [6], ammonia that in insects is converted into uric acid [49]. The two *D. melanogaster* GC isoforms have molecular masses close to 30 kDa and the tripartite structure and sequence motifs characteristic of the mitochondrial carrier family [1]. *Dm*GC1p and *Dm*GC2p share many transport properties. They both transport quite exclusively glutamate, are inactivated by the same inhibitors and have similar ΔpH dependence properties. However, they differ markedly in their kinetic parameters: the K_m values of *Dm*GC1p for glutamate are lower than those of *Dm*GC2p, and *Dm*GC2p is two times less active than *Dm*GC1p.

The expression profile observed across various *D. melanogaster* developmental stages, shows that *CG18347* is ubiquitous and probably has an essential role in the mitochondrial glutamate metabolism in *D. melanogaster*, as also confirmed by the observation that it is abundantly expressed in all the analyzed tissues. It is worth noting that its expression is particularly strong in the abdomen, where the fat bodies are mainly localized in the adult fly [50]. The energy storage role of this organ is well known in Drosophila as well as in other insects [51], and it is thought to be fundamental in the post-metamorphic energy metabolism. In contrast, the expression profile of the *CG12201* gene is strikingly different, showing a male specific expression confined to the testes. Flybase (http://flybase.org/) and FlyAtlas [52] expression data both support the peak of expression experimentally observed in the abdomen, with reported increased expression in the hindgut and in the larval fat bodies (not shown). Similarly, the testis specific expression of the *CG12201* gene is confirmed by microarray data reported in FlyAtlas.

In the light of the different kinetic parameters and tissue distribution of the two isoforms, it seems likely that *Dm*GC1p is responsible for the basic function of amino acid degradation, while *Dm*GC2p could become operative to accommodate the higher energy demand associated with specialized spermatozoa functions such as the capacitation process and the acrosome reaction [53]. Although at this stage a direct role of the *CG12201* product in spermatogenesis can only be speculated, the testis-specific expression is a feature of many gene duplicates in Drosophila [10]. This could be the basis of an intriguing mechanism leading to the evolution of novel gene functions following gene duplication events. We suggest that the expression of the gene duplicates can be initially confined to the male germline, and only later evolve into different expression patterns and potentially novel functions, as has also been proposed for duplicated genes in primates [54].

Furthermore, a potentially significant difference between the two *Dm*GC genes is in the presence of the NRG motif [45] in *CG18347* only analyzed for the first time in mitochondrial carrier family. The NRG site of the *D. melanogaster CG18347* gene, maintains the same subgenic position in all 20 Drosophilidae species studied and in its *G. morsitans* counterpart, although the surrounding noncoding sequences show remarkable divergence. The distribution, conservation and positioning of NRG sites strongly suggest that the glutamate carrier gene as well as the OXPHOS [45] genes are connected in a regulatory circuit in which this element plays a key role, and through which coordination of nuclear respiratory gene expression is accomplished. The inclusion of the glutamate carrier gene in the NRG circuit suggests its involvement in the management of the energy production, opening new avenues towards the functional study of mitochondrial biogenesis and bioenergetics in Drosophila and maybe in other species.

In mammals, the nuclear respiratory factors 1 and 2 (NRF1, NRF2), the peroxisome proliferative activated receptor α (PPAR α) and the Sp1 transcription factor have been characterized as transcriptional regulators of many genes involved in mitochondrial energy pathways, including a subset of the genes that encode subunits of the respiratory chain [55–58]. The target genes of NRF1 include constituents of the mtDNA transcription and replication machinery [56], suggesting that NRF1 has an important role in nuclear–mitochondrial communication. Interestingly, none of the target sites of these transcription factors overlaps with the NRG motif, and *D. melanogaster* has no obvious counterparts of NRF1, NRF2 or PPAR α, suggesting that mammals and invertebrates could base the control of energy production on different genetic circuits.

Comparative analysis of *Dm*GC1 and *Dm*GC2 coding sequences revealed that they share with human GCs the characteristic triplet set that defines the GC subfamily, with only a difference at the third position of triplet 22 where the aminoacids "GQS" were found in DmGC2p instead of "GQA" detected in *Dm*GC1p and human GCs [30]. Another important difference is at the level of the proposed binding site in correspondence of triplet 81 for which residues "IDL" are detected in *Dm*GC2p instead of "IDI" detected in DmGC1p and human GCs [30]. Three dimensional models of the two proteins were built by comparative modeling and residues involved in *DmGC1* and *DmGC2* substrate binding have been proposed.

Furthermore, it is speculated that the glutamate ligand in the *Dm*GC1p and *Dm*GC2p comparative models (Fig. 8) can interact with residues of the proposed binding sites and in particular with R195, D196, L91, I92 and R292 for *Dm*GC1p and R194, D195, L90, I91, and R287 for *Dm*GC2p. It is also speculated that the presence of an Ile residue (I296, triplet 81) in *Dm*GC1p instead of the Leu residue (L291, triplet 81) in *Dm*GC2p is able to reorient the Arg side-chain of triplet 77 (R292 for *Dm*GC1p, R287 for *Dm*GC2p) making possible a slightly different fitting of Glu within the carrier cavity of *Dm*GC1p at the proposed binding site level (see Fig. 8 models A and B). It is proposed that the Arg residue of triplet 77 should play a key role in the binding of glutamate in both proteins. It is interesting to highlight that proline at positions 206 and glycine at position 236 of SLC25A22_GC1, found mutated in the GC1 deficiency [8] (P206L and G236W), are conserved in both DmGC1 (P205 and G237) and DmGC2 (P204 and G236). Those residues were proposed to be involved in the uniport and exchange activity of the human GC1 [8] and most likely they play a similar role in Drosophila orthologs.

In the light of our results the metabolic role of glutamate carrier seems to be related to the energy demand with respect to amino acid degradation. When amino acids are used for energy production, toxic ammonia is produced. Glutamate and glutamine play critical roles acting as a kind of general collection point for amino groups. Ammonia is often converted in glutamate and transported to the liver and finally converted into urea. However, insects do not produce urea to detoxify ammonia, but convert ammonia to uric acid. In this system, intramitochondrially created ammonia is converted to glutamine by the action of glutamine synthetase (GS), and this is followed by synthesis of the excreted final product, uric acid [49]. Furthermore, in *D. melanogaster* high levels of glutamate in a cell cause an adverse effect and the excess of glutamate is removed by converting it to glutamine by GS [59]. The resulting increased level of glutamine will lead to the formation of megamitochondria that are induced in response to various intracellular or extracellular stresses [60]. In Drosophila, it has been demonstrated that glutamate transport or glutamate accumulation is a rate-limiting step for megamitochondrial formation and that GS1 apparently serves as a sensor of high levels of glutamate in the

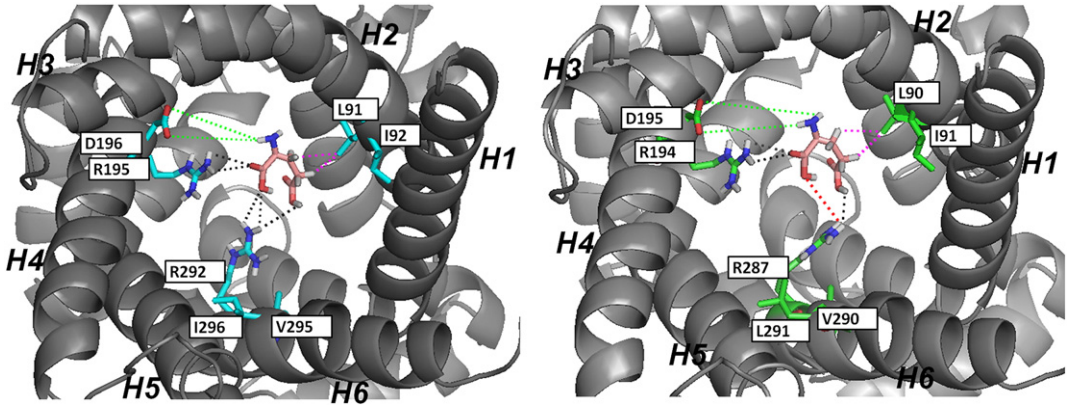

Fig. 8. Top view from the cytosolic side of the structural comparative models of Drosophila GC carriers highlighting the two carrier substrate binding sites. Panel A: Top view from the cytosolic side of the structural comparative model of *Dm*GC1p highlighting the carrier substrate binding site. Trans-membrane α-helices are gray colored and labeled from H1 to H6. The residues L91, I92, R195, D196, R292, V295 and I296 protruding into the cavity at the height of the binding site and the glutamate ligand are shown in stick representation. Panel B: Top view from the cytosolic side of the structural comparative model of *Dm*GC2p highlighting the carrier substrate binding site. The residues L90, I91, R194, D195, R287, V290 and L291 protruding into the cavity at the height of the binding site and the glutamate ligand are shown in stick representation. The PyMol (http://www.pymol.org/) color code used for both residues of the proposed binding site and glutamate ligand is: red, O-atoms; white, H-atoms; and blue, N-atoms. C-atoms in the labeled residues are colored in cyan and green in *Dm*GC1p and *Dm*GC2p respectively, whereas C-atoms of glutamate ligand are colored in pink. Glutamate docking poses were obtained by screening a gridbox involving residues of the predicted binding region located between the PG level 1 and PG level 2 areas [29] and by using Autodock 1.5.2. [64]. Possible interactions between the glutamate ligand and residues of the proposed binding sites are highlighted as follows: electrostatic/polar (black dashed lines), hydrophobic (purple dashed lines), potentially water-mediated interactions (green dashed lines) All the electrostatic/polar interactions depicted in the figure are in the range 3.1–3.5 Å within *Dm*GC1p and 2.6–3.6 Å within *Dm*GC2p. The red dashed line (4.8 Å) indicates the weakened polar interaction between glutamate ligand and R287 within *Dm*GC2p. All the hydrophobic interactions are in the range 3.2–3.4 Å within *Dm*GC1p and 3.3–3.7 Å within *Dm*GC2p. Potentially water-mediated interactions are in the range 8.5–9.5 Å both within *Dm*GC1p and *Dm*GC2p.

cell [61,62]. It should be noted that megamitochondria can also be produced by a high protein diet. Such high protein diets may cause an increase in intracellular amino acid levels and presumably in the level of glutamate. So, the *Dm*GCs could also play a key role in megamitochondrial formation and be involved in the control of nutritional stress.

In conclusion, *Dm*GC1p seems to be a main *D. melanogaster* glutamate carrier operating during uricogenesis, whereas *Dm*GC2p seems to be its paralog. Furthermore, the inclusion of the *Dm*GC1 gene in the NRG circuit reinforces its involvement in the management of the energy production, conversely the testis-specific expression of *Dm*GC2 suggests that it could be a gene in evolution that potentially will acquire a novel function, as has also been proposed for duplicated genes in primates.

Supplementary data to this article can be found online at http://dx.doi.org/10.1016/j.bbabio.2013.07.002.

References

[1] F. Palmieri, The mitochondrial transporter family SLC25: identification, properties and physiopathology, Mol. Aspects Med. 34 (2013) 465–484.
[2] G. Fiermonte, L. Palmieri, S. Todisco, G. Agrimi, F. Palmieri, J.E. Walker, Identification of the mitochondrial glutamate transporter. Bacterial expression, reconstitution, functional characterization, and tissue distribution of two human isoforms, J. Biol. Chem. 277 (2002) 19289–19294.
[3] F. Palmieri, Diseases caused by defects of mitochondrial carriers: a review, Biochim. Biophys. Acta 1777 (2008) 564–578.
[4] K.F. LaNoue, A.C. Schoolwerth, Metabolite transport in mitochondria, Annu. Rev. Biochem. 48 (1979) 871–922.
[5] M. Casimir, F.M. Lasorsa, B. Rubi, D. Caille, F. Palmieri, P. Meda, P. Maechler, Mitochondrial glutamate carrier GC1 as a newly identified player in the control of glucose-stimulated insulin secretion, J. Biol. Chem. 284 (2009) 25004–25014.
[6] N.M. Bradford, J.D. McGivan, Quantitative characteristics of glutamate transport in rat liver mitochondria, Biochem. J. 134 (1973) 1023–1029.
[7] J. Meyer, P.M. Vignais, Kinetic study of glutamate transport in rat liver mitochondria, Biochim. Biophys. Acta 325 (1973) 375–384.
[8] F. Molinari, A. Raas-Rothschild, M. Rio, G. Fiermonte, F. Encha-Razavi, L. Palmieri, F. Palmieri, Z. Ben-Neriah, N. Kadhom, M. Vekemans, T. Attie-Bitach, A. Munnich, P. Rustin, L. Colleaux, Impaired mitochondrial glutamate transport in autosomal recessive neonatal myoclonic epilepsy, Am. J. Hum. Genet. 76 (2005) 334–339.
[9] G. Moreno-Hagelsieb, K. Latimer, Choosing BLAST options for better detection of orthologs as reciprocal best hits, Bioinformatics 24 (2008) 319–324.
[10] D. Porcelli, P. Barsanti, G. Pesole, C. Caggese, The nuclear OXPHOS genes in insecta: a common evolutionary origin, a common *cis*-regulatory motif, a common destiny for gene duplicates, BMC Evol. Biol. 7 (2007) 215.
[11] V. Dolce, P. Scarcia, D. Iacopetta, F. Palmieri, A fourth ADP/ATP carrier isoform in man: identification, bacterial expression, functional characterization and tissue distribution, FEBS Lett. 579 (2005) 633–637.
[12] D. Iacopetta, C. Carrisi, G. De Filippis, V.M. Calcagnile, A.R. Cappello, A. Chimento, R. Curcio, A. Santoro, A. Vozza, V. Dolce, F. Palmieri, L. Capobianco, The biochemical properties of the mitochondrial thiamine pyrophosphate carrier from *Drosophila melanogaster*, FEBS J. 277 (2010) 1172–1181.
[13] C. Carrisi, M. Madeo, P. Morciano, V. Dolce, G. Cenci, A.R. Cappello, G. Mazzeo, D. Iacopetta, L. Capobianco, Identification of the *Drosophila melanogaster* mitochondrial citrate carrier: bacterial expression, reconstitution, functional characterization and developmental distribution, J. Biochem. 144 (2008) 389–392.
[14] L. Palmieri, V. De Marco, V. Iacobazzi, F. Palmieri, M.J. Runswick, J.E. Walker, Identification of the yeast ARG-11 gene as a mitochondrial ornithine carrier involved in arginine biosynthesis, FEBS Lett. 410 (1997) 447–451.
[15] L. Palmieri, F. Palmieri, M.J. Runswick, J.E. Walker, Identification by bacterial expression and functional reconstitution of the yeast genomic sequence encoding the mitochondrial dicarboxylate carrier protein, FEBS Lett. 399 (1996) 299–302.
[16] M. Madeo, C. Carrisi, D. Iacopetta, L. Capobianco, A.R. Cappello, C. Bucci, F. Palmieri, G. Mazzeo, A. Montalto, V. Dolce, Abundant expression and purification of biologically active mitochondrial citrate carrier in baculovirus-infected insect cells, J. Bioenerg. Biomembr. 41 (2009) 289–297.
[17] V. Dolce, G. Fiermonte, M.J. Runswick, F. Palmieri, J.E. Walker, The human mitochondrial deoxynucleotide carrier and its role in the toxicity of nucleoside antivirals, Proc. Natl. Acad. Sci. U. S. A. 98 (2001) 2284–2288.
[18] C.M. Marobbio, A. Vozza, M. Harding, F. Bisaccia, F. Palmieri, J.E. Walker, Identification and reconstitution of the yeast mitochondrial transporter for thiamine pyrophosphate, EMBO J. 21 (2002) 5653–5661.
[19] F. Palmieri, C. Indiveri, F. Bisaccia, V. Iacobazzi, Mitochondrial metabolite carrier proteins: purification, reconstitution, and transport studies, Methods Enzymol. 260 (1995) 349–369.
[20] G. Fiermonte, V. Dolce, L. David, F.M. Santorelli, C. Dionisi-Vici, F. Palmieri, J.E. Walker, The mitochondrial ornithine transporter. Bacterial expression, reconstitution, functional characterization, and tissue distribution of two human isoforms, J. Biol. Chem. 278 (2003) 32778–32783.
[21] F. Bisaccia, C. Indiveri, F. Palmieri, Purification of reconstitutively active alpha-oxoglutarate carrier from pig heart mitochondria, Biochim. Biophys. Acta 810 (1985) 362–369.
[22] F. Bisaccia, A. De Palma, F. Palmieri, Identification and purification of the tricarboxylate carrier from rat liver mitochondria, Biochim. Biophys. Acta 977 (1989) 171–176.
[23] A. Santoro, A.R. Cappello, M. Madeo, E. Martello, D. Iacopetta, V. Dolce, Interaction of fosfomycin with the glycerol 3-phosphate transporter of *Escherichia coli*, Biochim. Biophys. Acta 1810 (2011) 1323–1329.
[24] D. Bonofiglio, A. Santoro, E. Martello, D. Vizza, D. Rovito, A.R. Cappello, I. Barone, C. Giordano, S. Panza, S. Catalano, V. Iacobazzi, V. Dolce, S. Ando, Mechanisms of divergent effects of activated Peroxisome Proliferator-Activated Receptor-gamma on mitochondrial Citrate Carrier expression in 3T3-L1 fibroblasts and mature adipocytes, Biochim. Biophys. Acta 1831 (2013) 1027–1036.
[25] F. Palmieri, M. Klingenberg, Direct methods for measuring metabolite transport and distribution in mitochondria, Methods Enzymol. 56 (1979) 279–301.
[26] K.J. Livak, T.D. Schmittgen, Analysis of relative gene expression data using real-time quantitative PCR and the 2(−delta delta c(t)) method, Methods 25 (2001) 402–408.

[27] C.L. Pierri, G. Parisi, V. Porcelli, Computational approaches for protein function prediction: a combined strategy from multiple sequence alignment to molecular docking-based virtual screening, Biochim. Biophys. Acta 1804 (2011) 1695–1712.
[28] E. Pebay-Peyroula, C. Dahout-Gonzalez, R. Kahn, V. Trezeguet, G.J. Lauquin, G. Brandolin, Structure of mitochondrial ADP/ATP carrier in complex with carboxyatractyloside, Nature 426 (2003) 39–44.
[29] F. Palmieri, C.L. Pierri, Structure and function of mitochondrial carriers — role of the transmembrane helix P and G residues in the gating and transport mechanism, FEBS Lett. 584 (2010) 1931–1939.
[30] F. Palmieri, C.L. Pierri, A. De Grassi, A. Nunes-Nesi, A.R. Fernie, Evolution, structure and function of mitochondrial carriers: a review with new insights, Plant J. 66 (2011) 161–181.
[31] A.R. Cappello, R. Curcio, D. Valeria Miniero, I. Stipani, A.J. Robinson, E.R. Kunji, F. Palmieri, Functional and structural role of amino acid residues in the even-numbered transmembrane alpha-helices of the bovine mitochondrial oxoglutarate carrier, J. Mol. Biol. 363 (2006) 51–62.
[32] A.R. Cappello, D.V. Miniero, R. Curcio, A. Ludovico, L. Daddabbo, I. Stipani, A.J. Robinson, E.R. Kunji, F. Palmieri, Functional and structural role of amino acid residues in the odd-numbered transmembrane alpha-helices of the bovine mitochondrial oxoglutarate carrier, J. Mol. Biol. 369 (2007) 400–412.
[33] C.M. Marobbio, G. Giannuzzi, E. Paradies, C.L. Pierri, F. Palmieri, alpha-Isopropylmalate, a leucine biosynthesis intermediate in yeast, is transported by the mitochondrial oxalacetate carrier, J. Biol. Chem. 283 (2008) 28445–28453.
[34] G. Fiermonte, V. Dolce, L. Palmieri, M. Ventura, M.J. Runswick, F. Palmieri, J.E. Walker, Identification of the human mitochondrial oxodicarboxylate carrier. Bacterial expression, reconstitution, functional characterization, tissue distribution, and chromosomal location, J. Biol. Chem. 276 (2001) 8225–8230.
[35] G. Fiermonte, L. Palmieri, V. Dolce, F.M. Lasorsa, F. Palmieri, M.J. Runswick, J.E. Walker, The sequence, bacterial expression, and functional reconstitution of the rat mitochondrial dicarboxylate transporter cloned via distant homologs in yeast and *Caenorhabditis elegans*, J. Biol. Chem. 273 (1998) 24754–24759.
[36] L. Palmieri, G. Agrimi, M.J. Runswick, I.M. Fearnley, F. Palmieri, J.E. Walker, Identification in *Saccharomyces cerevisiae* of two isoforms of a novel mitochondrial transporter for 2-oxoadipate and 2-oxoglutarate, J. Biol. Chem. 276 (2001) 1916–1922.
[37] L. Capobianco, F. Bisaccia, M. Mazzeo, F. Palmieri, The mitochondrial oxoglutarate carrier: sulfhydryl reagents bind to cysteine-184, and this interaction is enhanced by substrate binding, Biochemistry 35 (1996) 8974–8980.
[38] L. Palmieri, F.M. Lasorsa, V. Iacobazzi, M.J. Runswick, F. Palmieri, J.E. Walker, Identification of the mitochondrial carnitine carrier in *Saccharomyces cerevisiae*, FEBS Lett. 462 (1999) 472–476.
[39] F. Palmieri, B. Rieder, A. Ventrella, E. Blanco, P.T. Do, A. Nunes-Nesi, A.U. Trauth, G. Fiermonte, J. Tjaden, G. Agrimi, S. Kirchberger, E. Paradies, A.R. Fernie, H.E. Neuhaus, Molecular identification and functional characterization of *Arabidopsis thaliana* mitochondrial and chloroplastic NAD+ carrier proteins, J. Biol. Chem. 284 (2009) 31249–31259.
[40] L. Palmieri, N. Picault, R. Arrigoni, E. Besin, F. Palmieri, M. Hodges, Molecular identification of three *Arabidopsis thaliana* mitochondrial dicarboxylate carrier isoforms: organ distribution, bacterial expression, reconstitution into liposomes and functional characterization, Biochem. J. 410 (2008) 621–629.
[41] C.M. Marobbio, M.A. Di Noia, F. Palmieri, Identification of a mitochondrial transporter for pyrimidine nucleotides in *Saccharomyces cerevisiae*: bacterial expression, reconstitution and functional characterization, Biochem. J. 393 (2006) 441–446.
[42] F. Palmieri, C. Indiveri, F. Bisaccia, R. Kramer, Functional properties of purified and reconstituted mitochondrial metabolite carriers, J. Bioenerg. Biomembr. 25 (1993) 525–535.
[43] S.T. Smale, J.T. Kadonaga, The RNA polymerase II core promoter, Annu. Rev. Biochem. 72 (2003) 449–479.
[44] M. Thomas-Chollier, M. Defrance, A. Medina-Rivera, O. Sand, C. Herrmann, D. Thieffry, J. van Helden, RSAT 2011: regulatory sequence analysis tools, Nucleic Acids Res. 39 (2011) W86–W91.
[45] M. Sardiello, G. Tripoli, A. Romito, C. Minervini, L. Viggiano, C. Caggese, G. Pesole, Energy biogenesis: one key for coordinating two genomes, Trends Genet. 21 (2005) 12–16.
[46] P. Rehm, J. Borner, K. Meusemann, B.M. von Reumont, S. Simon, H. Hadrys, B. Misof, T. Burmester, Dating the arthropod tree based on large-scale transcriptome data, Mol. Phylogenet. Evol. 61 (2011) 880–887.
[47] A.J. Robinson, C. Overy, E.R. Kunji, The mechanism of transport by mitochondrial carriers based on analysis of symmetry, Proc. Natl. Acad. Sci. U. S. A. 105 (2008) 17766–17771.
[48] A.J. Robinson, E.R. Kunji, Mitochondrial carriers in the cytoplasmic state have a common substrate binding site, Proc. Natl. Acad. Sci. U. S. A. 103 (2006) 2617–2622.
[49] J.E. Vorhaben, J.W. Campbell, Glutamine synthetase. A mitochondrial enzyme in uricotelic species, J. Biol. Chem. 247 (1972) 2763–2767.
[50] J.R. Aguila, J. Suszko, A.G. Gibbs, D.K. Hoshizaki, The role of larval fat cells in adult *Drosophila melanogaster*, J. Exp. Biol. 210 (2007) 956–963.
[51] D.K. Hoshizaki, Fat-cell development, Complete Molecular Insect Science, 2, 2005, pp. 315–345.
[52] V.R. Chintapalli, J. Wang, J.A. Dow, Using FlyAtlas to identify better *Drosophila melanogaster* models of human disease, Nat. Genet. 39 (2007) 715–720.
[53] A.R. Cappello, C. Guido, A. Santoro, M. Santoro, L. Capobianco, D. Montanaro, M. Madeo, S. Ando, V. Dolce, S. Aquila, The mitochondrial citrate carrier (CIC) is present and regulates insulin secretion by human male gamete, Endocrinology 153 (2012) 1743–1754.
[54] N. Vinckenbosch, I. Dupanloup, H. Kaessmann, Evolutionary fate of retroposed gene copies in the human genome, Proc. Natl. Acad. Sci. U. S. A. 103 (2006) 3220–3225.
[55] R.C. Scarpulla, Transcriptional activators and coactivators in the nuclear control of mitochondrial function in mammalian cells, Gene 286 (2002) 81–89.
[56] D.P. Kelly, R.C. Scarpulla, Transcriptional regulatory circuits controlling mitochondrial biogenesis and function, Genes Dev. 18 (2004) 357–368.
[57] R. Li, K. Luciakova, B.D. Nelson, Expression of the human cytochrome c_1 gene is controlled through multiple Sp1-binding sites and an initiator region, Eur. J. Biochem. 241 (1996) 649–656.
[58] T. Gulick, S. Cresci, T. Caira, D.D. Moore, D.P. Kelly, The peroxisome proliferator-activated receptor regulates mitochondrial fatty acid oxidative enzyme gene expression, Proc. Natl. Acad. Sci. U. S. A. 91 (1994) 11012–11016.
[59] C. Caggese, P. Barsanti, L. Viggiano, M.P. Bozzetti, R. Caizzi, Genetic, molecular and developmental analysis of the glutamine synthetase isozymes of *Drosophila melanogaster*, Genetica 94 (1994) 275–281.
[60] T. Wakabayashi, Megamitochondria formation — physiology and pathology, J. Cell Mol. Med. 6 (2002) 497–538.
[61] M.S. Shim, J.Y. Kim, K.H. Lee, H.K. Jung, B.A. Carlson, X.M. Xu, D.L. Hatfield, B.J. Lee, l(2)01810 is a novel type of glutamate transporter that is responsible for megamitochondrial formation, Biochem. J. 439 (2011) 277–286.
[62] M.S. Shim, J.Y. Kim, H.K. Jung, K.H. Lee, X.M. Xu, B.A. Carlson, K.W. Kim, I.Y. Kim, D.L. Hatfield, B.J. Lee, Elevation of glutamine level by selenophosphate synthetase 1 knockdown induces megamitochondrial formation in Drosophila cells, J. Biol. Chem. 284 (2009) 32881–32894.
[63] F. Palmieri, C.L. Pierri, Mitochondrial metabolite transport, Essays Biochem. 47 (2010) 37–52.
[64] G.M. Morris, R. Huey, W. Lindstrom, M.F. Sanner, R.K. Belew, D.S. Goodsell, A.J. Olson, AutoDock4 and AutoDockTools4: automated docking with selective receptor flexibility, J. Comput. Chem. 30 (2009) 2785–2791.